Journal of Physics: Conference Series **668** (2016) 012078 doi:10.1088/1742-6596/668/1/012078

Charged particle production in Pb-Pb and p-Pb collisions measured by the ATLAS detector

Evgeny Shulga for the ATLAS collaboration

National Research Nuclear University "MEPhI", Kashirskoe shosse 31, Moscow, Russian Federation

E-mail: eshulga@cern.ch

Abstract. The ATLAS experiment at the Large Hadron Collider measures charged hadron spectra in Pb+Pb and p+Pb collisions. The results are compared to the pp spectra of charged hadrons at the same centre-of-mass energy. Charged hadron distributions from Pb+Pb are compared to charged particle cross-sections in pp collisions at $\sqrt{s} = 2.76$ TeV, reference cross-section for p+Pb at $\sqrt{s_{NN}} = 5.02$ TeV is reconstructed using $\sqrt{s} = 2.76$ TeV and 7 TeV pp results. These allow for a detailed comparison of the collision systems in a wide transverse momentum and rapidity ranges in different centrality intervals. The nuclear modification factors $R_{\rm AA}$ and $R_{\rm pPb}$ are presented as a function of centrality, $p_{\rm T}$, η. The charged particle $R_{\rm AA}$ is found to vary significantly as a function of transverse momentum, and shows a pronounced minimum at about 7 GeV. Above 60 GeV, $R_{\rm AA}$ is consistent with a flat, centrality-dependent, value within the uncertainties. $R_{\rm pPb}$ results show strong rapidity dependence in the region of so-called Cronin peak at about 2 GeV and above $p_{\rm T}$ of 10 GeV show anomalous enhancement.

ATL-PHYS-PROC-2015-070
14 September 2015

1. Introduction

Charged hadrons of high transverse momentum ($p_{\rm T}$) are a tool that can be used to study strongly interacting matter [1, 2] produced in high-energy heavy-ion collisions (Pb+Pb). It is expected from first results of the LHC experiments [3–5] that the resulting spectrum of hadrons, which originate from parton fragmentation [6, 7], is modified. Additionally proton-nucleus (p+Pb) collisions probe the physics of the initial state of ultra-relativistic heavy ion collisions without the effects of thermalization, playing an important role in Pb+Pb collisions evolution [8]. p+Pb spectra can provide insight on the effect of an extended nuclear target on the dynamics of soft and hard scattering processes and subsequent particle production. For an extensive review of predictions see [9].

2. Analysis

For Pb+Pb and p+Pb collisions the expected particle production rate can be quantified using the "nuclear modification factor" which is calculated as the ratio of differential yield of charged particles in Pb+Pb or p+Pb collisions divided by the average value of the nuclear thickness function $\langle T_{\rm Pb} \rangle$ (in units of inverse barns) [10] and differential charged-particle production cross section measured in pp collisions. Differential yield of charged particles can be measured as a function of centrality, eta, y (or $y^\star$ in case of p+Pb, which due to different beam energies has its centre-of-mass system boosted by -0.465 [11]).

This proceedings presents a high-statistics measurement of charged-hadron spectra, $R_{\rm AA}$ and $R_{\rm pPb}$ as a function of $p_{\rm T}$ and intervals of collision centrality for $0.5 < p_{\rm T} < 150$ GeV. The collision centrality is estimated using the sum of transverse energy measured in the ATLAS [12] forward calorimeter, $3.1 < |\eta| < 4.9$, in both parts of the detector for Pb+Pb [13] and only in the outgoing Pb beam direction for p+Pb [10], the dependence of p+Pb collisions on the number of participating nucleons ($N_{\rm part}$) was estimated using two models: the Glauber model [14] and the Glauber-Gribov colour-fluctuation approach [15], with the relative fluctuations determined by the parameter Ω. Pb+Pb data recorded by the ATLAS experiment in the 2010 and 2011 HI physics runs of the LHC at $\sqrt{s} = 2.76$ TeV, and the pp data at the same value of $\sqrt{s}$ recorded in the 2011 and 2013 physics runs. The total integrated luminosity of the combined Pb+Pb sample is $0.15\,{\rm nb}^{-1}$, and that of the combined pp sample is $4.2\,{\rm pb}^{-1}$. The proton-proton data sets used to obtain reference measurement for p+Pb results at $\sqrt{s} = 7$ TeV with total integrated luminosity 130 $\mu{\rm b}^{-1}$ were obtained in April 2010. For p+Pb studies events were preselected within the vertex range $|z_{\rm vtx}| < 150$ mm, and at least one hit in each of the MBTS detectors. In addition, a time difference of less than 10 ns was required between the two MBTS sides.

The events used in this analysis are selected from several triggered samples. A minimum bias (MB) samples were obtained requiring signal in the Minimum Bias Trigger Scintillator. For jet triggered samples, jets were reconstructed in events that passed the MB requirement using the anti-kt algorithm [16] with the distance parameter R=0.4. Events were selected by the jet trigger if they contained jets with $E_{\rm T}$ above a certain threshold. Multiple thresholds were defined. Only a fraction of all events which fired a trigger was randomly selected to be recorded for further analysis. This fraction was set differently for each trigger. Total spectra were obtained by merging spectra from MB and jet triggers, all of them scaled by reciprocal of the fraction to obtain MB spectra up to high $p_{\rm T}$ [17].

Charge particle tracks are reconstructed in the ATLAS Inner Detector [13]. Tracks are measured using a combination of silicon pixel detector (Pixel), silicon microstrip detector (SCT), and a straw tube transition radiation tracker (TRT), all immersed in a 2 T axial magnetic field. Charged particles typically traverse 3 layers of silicon pixel detectors, 4 layers of double sided microstrip detector, and 36 straws. Each track is required to have at least 1 hit in the Pixel detector, a hit in the innermost layer if such hit is expected by the tracking model, and at least 6 hits in the SCT. Additionally, tracks with $p_{\rm T} > 10$ GeV are required to produce at least 8 hits in the TRT. These requirements select tracks with good $p_{\rm T}$ resolution and suppress the contribution of poorly reconstructed tracks. Yet they limit the analysis to the coverage of the TRT detector, thus all tracks are selected with $|\eta| < 2$. To ensure that the tracks originate from the event vertex of Pb+Pb(p+Pb) collisions, the transverse impact parameter, d_0, and $z_0 sin\theta$ (z_0 is the longitudinal impact parameter) are required to be less than 3(1.5) mm. Tracks selected for the analysis are also required to satisfy the conditions on the impact parameters significances: $|d0/\sigma d_0| < 3$ and $|z_0 sin\theta/\sigma z_0 sin\theta| < 3$. The d_0 and $z_0 sin\theta$ parameters and their uncertainties are estimated by a vertex finding algorithm. The jet is reconstructed with a radius parameter of $\Delta R = 0.2$ in Pb+Pb and $\Delta R = 0.4$ in p+Pb and pp collisions. The track-to-jet matching requirement is applied to all tracks with $p_{\rm T} > 15$ GeV in p+Pb and pp collisions and $p_{\rm T} > 20$ GeV in Pb+Pb collisions both in the MB and jet-triggered samples, to reduce the amount of mis-measured tracks at high $p_{\rm T}$. Tracks associated with electrons and muons with $p_{\rm T}$ above 10 GeV coming predominately from electroweak decays bosons are subtracted from the measured spectra. Reconstructed charged particle spectra in different collision systems are corrected for mis-measured tracks and secondary particles, for limited momentum resolution, and for tracking inefficiency. The resulting spectra are unfolded using the iterative Bayesian unfolding [18] to correct for the finite detector $p_{\rm T}$ resolution.

Once the differential pp cross section at $\sqrt{s}$=2.76 and 7 TeV have been measured, the differential pp cross section at $\sqrt{s_{NN}}$=5.02 TeV is obtained by interpolation. The interpolation

is proportional to $\ln(\sqrt{s})$ and it is performed for every p_{T} bin in each rapidity interval used in the p+Pb analysis.

3. Results

Figure 1(left) shows the nuclear modification factor R_{AA} as a function of p_{T} in five centrality intervals. The R_{AA} measured as a function of p_{T} shows a characteristic non-flat p_{T} shape which becomes more pronounced for more central collisions. In all centrality and rapidity intervals studied the R_{AA}shows a characteristic shape with a local maximum at $p_{\mathrm{T}} \approx 2$ GeV decreasing to a minimum at $p_{\mathrm{T}} \approx 7$ GeV. It increases again towards higher p_{T} with a change in the slope at $p_{\mathrm{T}} \approx 60$ GeV, where the rise becomes much less steep. Above this p_{T}, the p_{T} dependence is consistent with a flat behaviour within statistical and systematic uncertainties. This shape is present in all measured centrality and pseudorapidity intervals, but it has the largest maximum-to-minimum ratio in the most central collisions. Figure 1(right) shows R_{AA} as a function of the mean number of participating nucleons, $\langle N_{\mathrm{part}} \rangle$, in the four momentum intervals corresponding to the local maximum, local minimum, plateau and intermediate region of R_{AA} values. Overall decrease of R_{AA} with $\langle N_{\mathrm{part}} \rangle$ is pronounced, the dependence is strongest around the minimum of R_{AA} ($p_{\mathrm{T}} \approx 7$ GeV) and weakest in the p_{T} region above 60 GeV [19].

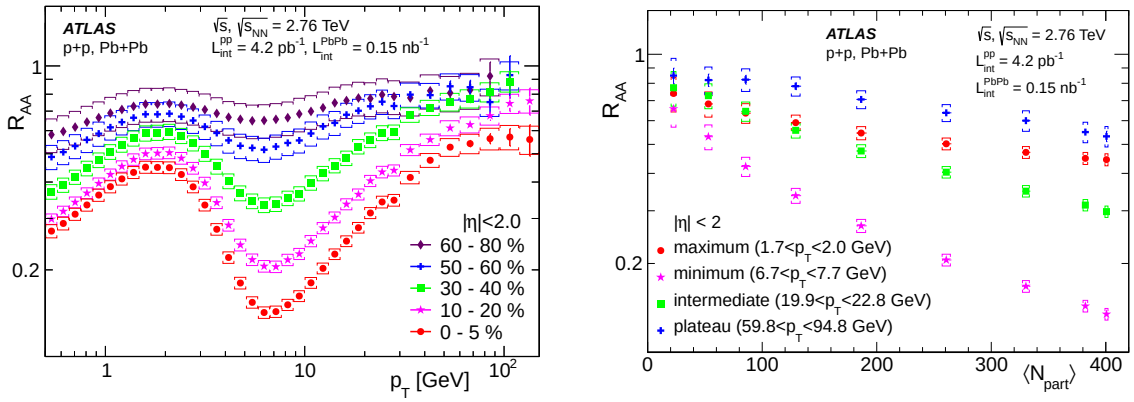

Figure 1: (left) The R_{AA} as a function of p_{T} measured in five centrality intervals $0-5\%$, $10-20\%$, $30-40\%$, $50-60\%$ and $60-80\%$. (right) The R_{AA} as a function of $\langle N_{\mathrm{part}} \rangle$ for four p_{T} intervals corresponding to the maximum R_{AA} ($1.7 < p_{\mathrm{T}} < 2.0 GeV$), minimum R_{AA}($6.7 < p_{\mathrm{T}} < 7.7 GeV$), intermediate R_{AA} ($19.9 < p_{\mathrm{T}} < 22.8 GeV$) and plateau of R_{AA} ($59.8 < p_{\mathrm{T}} < 94.8 GeV$). The statistical uncertainties, which are smaller than the size of markers in all but a few cases, are shown with vertical bars and the systematic uncertainties with brackets.

Figure 2 shows the R_{pPb} distributions for 2 centrality classes ($0-10\%$ and $60-90\%$) and for the rapidity interval $-1.5 < y^{\star} < 2$.The nuclear modification factors increase with momentum in the region $0.1 < p_{\mathrm{T}} < 2$ GeV, then reach a maximum and decrease up to $p_{\mathrm{T}} \approx 8$ GeV. Above that momentum the nuclear modification factor is constant within the experimental uncertainties. The magnitude of the peak strongly depends both on rapidity and centrality. It increases from peripheral to the central collisions and from the proton beam direction to the Pb beam direction [11]. The choice of the different geometrical model strongly affects the level of the plateau in the central events and its magnitude with respect to peripheral. Higher p_{T} ranges have been also measured, showing a clear trend of increasing enhancement towards higher p_{T}. This trend does not have a strong rapidity dependence but is more marked in peripheral events [17]. The results for high p_{T} measurement seem to show the same trend at high p_{T} as was observed by the CMS collaboration [20] but not the ALICE collaboration [21].

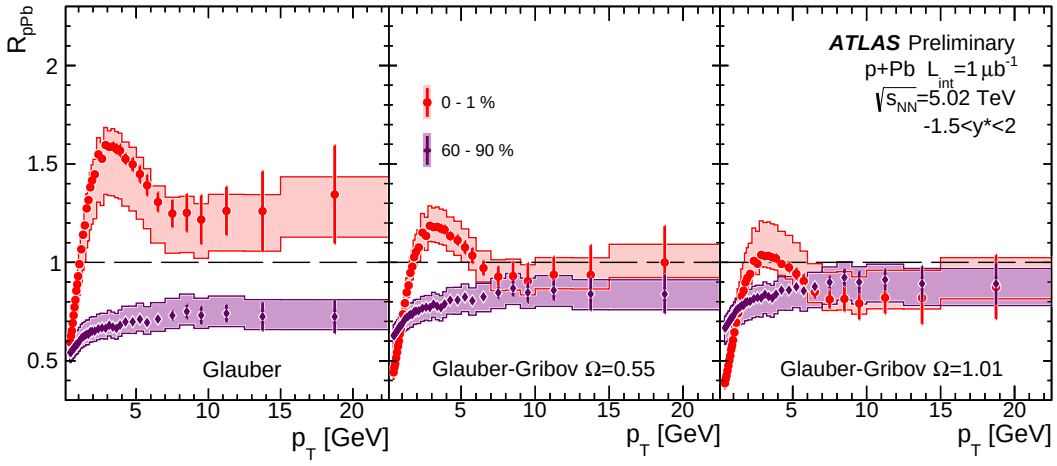

Figure 2: $R_{\rm pPb}$ as a function of $p_{\rm T}$ extracted from the invariant yields integrated over $-1.5 < y^{\star} < 2$ for the $0-1\%$ and $60-90\%$ centrality intervals, and for the three different geometrical models from left to right (Glauber, Glauber-Gribov $\Omega = 0.55$ and Glauber-Gribov $\Omega = 1.01$). Statistical errors are indicated with vertical lines and the systematic uncertainties on the invariant yields are indicated by a shaded area. The total systematic uncertainty, which includes the uncertainty on $\langle T_{\rm pA} \rangle$ or its ratios are indicated by lines of the same colour.

4. Acknowledgements

This research is supported by The Ministry of education and science of Russian Federation, project 3.472.2014/K.

References

[1] D. G. d'Enterria, Eur. Phys. J. **C43** (2005) 295–302, arXiv:nucl-ex/0504001 [nucl-ex].
[2] J. Casalderrey-Solana and C. A. Salgado, Acta Phys. Polon. **B38** (2007) 3731–3794, arXiv:0712.3443 [hep-ph].
[3] ATLAS Collaboration, Phys. Rev. Lett. **105** (2010) 252303, arXiv:1011.6182 [hep-ex].
[4] CMS Collaboration, Phys. Rev. **C84** (2011) 024906, arXiv:1102.1957 [nucl-ex].
[5] ALICE Collaboration, J. Adam et al., Phys. Lett. **B746** (2015) 1–14, arXiv:1502.01689 [nucl-ex].
[6] ATLAS Collaboration, Phys. Lett. **B739** (2014) 320–342, arXiv:1406.2979 [hep-ex].
[7] CMS Collaboration, Phys. Rev. **C90** no. 2, (2014) 024908, arXiv:1406.0932 [nucl-ex].
[8] L. P. Csernai, J. I. Kapusta, and L. D. McLerran, Phys. Rev. Lett. **97** (2006) 152303, arXiv:nucl-th/0604032.
[9] J. Albacete, N. Armesto, R. Baier, G. Barnafoldi, J. Barrette, et al., Int.J.Mod.Phys. **E22** (2013) 1330007, arXiv:1301.3395.
[10] ATLAS Collaboration, arXiv:1508.00848 [hep-ex].
[11] Tech. Rep. ATLAS-CONF-2013-107, CERN, Geneva, Nov, 2013.
[12] ATLAS Collaboration, JINST **3** (2008) S08003.
[13] ATLAS Collaboration, Phys. Lett. **B707** (2012) 330–348, arXiv:1108.6018 [hep-ex].
[14] M. L. Miller, K. Reygers, S. J. Sanders, and P. Steinberg, Ann. Rev. Nucl. Part. Sci. **57** (2007) 205–243, arXiv:nucl-ex/0701025 [nucl-ex].
[15] M. Alvioli and M. Strikman, Phys. Lett. **B722** (2013) 347–354, arXiv:1301.0728.
[16] M. Cacciari, G. P. Salam, and G. Soyez, JHEP **04** (2008) 063, arXiv:0802.1189 [hep-ph].
[17] Tech. Rep. ATLAS-CONF-2014-029, CERN, Geneva, May, 2014.
[18] ATLAS Collaboration, arXiv:1104.2962 [hep-ex].
[19] ATLAS Collaboration, arXiv:1504.04337 [hep-ex].
[20] CMS Collaboration, Eur. Phys. J. **C75** no. 5, (2015) 237, arXiv:1502.05387 [nucl-ex].
[21] ALICE Collaboration, B. B. Abelev et al., Eur. Phys. J. **C74** no. 9, (2014) 3054, arXiv:1405.2737 [nucl-ex].